

ACCEPTED MANUSCRIPT • OPEN ACCESS

Data assimilation finite element method for the linearized Navier-Stokes equations in the low Reynolds regime

To cite this article before publication: Muriel Boulakia *et al* 2020 *Inverse Problems* in press <https://doi.org/10.1088/1361-6420/ab9161>

Manuscript version: Accepted Manuscript

Accepted Manuscript is “the version of the article accepted for publication including all changes made as a result of the peer review process, and which may also include the addition to the article by IOP Publishing of a header, an article ID, a cover sheet and/or an ‘Accepted Manuscript’ watermark, but excluding any other editing, typesetting or other changes made by IOP Publishing and/or its licensors”

This Accepted Manuscript is © 2020 The Author(s). Published by IOP Publishing Ltd..

As the Version of Record of this article is going to be / has been published on a gold open access basis under a CC BY 3.0 licence, this Accepted Manuscript is available for reuse under a CC BY 3.0 licence immediately.

Everyone is permitted to use all or part of the original content in this article, provided that they adhere to all the terms of the licence <https://creativecommons.org/licenses/by/3.0>

Although reasonable endeavours have been taken to obtain all necessary permissions from third parties to include their copyrighted content within this article, their full citation and copyright line may not be present in this Accepted Manuscript version. Before using any content from this article, please refer to the Version of Record on IOPscience once published for full citation and copyright details, as permissions may be required. All third party content is fully copyright protected and is not published on a gold open access basis under a CC BY licence, unless that is specifically stated in the figure caption in the Version of Record.

View the [article online](#) for updates and enhancements.

1
2
3
4
5
6
7
8
9
10
11 Data assimilation finite element method for the
12 linearized Navier-Stokes equations in the low
13 Reynolds regime
14
15
16
17

18 Muriel Boulakia^{†,*}, Erik Burman[‡], Miguel A. Fernández^{*,†}, and
19 Colette Voisembert^{*,†}
20

21 [†]Sorbonne Université & CNRS, UMR 7598 LJLL, 75005 Paris, France

22 ^{*}Inria Paris, 75012 Paris, France

23 [‡]Department of Mathematics, University College London,
24 London WC1E 6BT, United Kingdom
25
26

27
28 May 1, 2020
29
30

31 **Abstract**

32
33 In this paper, we are interested in designing and analyzing a finite
34 element data assimilation method for laminar steady flow described
35 by the linearized incompressible Navier-Stokes equation. We propose
36 a weakly consistent stabilized finite element method which reconstructs
37 the whole fluid flow from noisy velocity measurements in a subset of the
38 computational domain. Using the stability of the continuous problem
39 in the form of a three balls inequality, we derive quantitative local
40 error estimates for the velocity. Numerical simulations illustrate these
41 convergence properties and we finally apply our method to the flow
42 reconstruction in a blood vessel.
43

44 **1 Introduction**
45

46 The question of how to assimilate measured data into large scale compu-
47 tations of flow problems is receiving increasing attention from the compu-
48 tational community. There are several different situations where such data
49 assimilation problems arise. One situation is when the data necessary to
50 make the flow problem well posed is lacking, for instance when boundary
51 data can not be obtained on parts of the boundary, but some other measured
52
53
54
55
56
57
58
59
60

1
2
3
4
5
6
7
8 data on the boundary or in the bulk is available to make up for this short-
9 fall. In such situation, the problem is ill-posed and numerical simulations
10 are much more delicate to handle than for the well-posed flow equations.
11 The traditional approach is to regularize the continuous problem to obtain
12 a well-posed continuous problem, often using a variational framework, that
13 can then be discretized using standard techniques. The regularization pa-
14 rameter then has to be tuned to have an optimal value with respect to noise
15 in the data. The granularity of the computational mesh is chosen afterwards
16 to resolve all scales of the regularized problem. An example of this strategy
17 is the quasi-reversibility method (see the references [8, 9, 10, 11]) which is
18 applied to Stokes problem in [10] for the inverse identification of bound-
19 aries. Other examples can be found in [26], where additional measured data
20 is used to compensate for a lack of knowledge of the boundary conditions
21 in hemodynamics, or in [35], where a least squares method is proposed for
22 combining and enhancing the results from an existing computational fluid
23 dynamics model with experimental data. More generally the variational
24 data assimilation method dates back to the work of Sasaki [38] where it was
25 introduced in the context of meteorology. For further developments, we re-
26 fer for example to [41, 40]. Other approaches to data assimilation exist such
27 as nudging [32, 2, 30] or minimax estimates [42]. The upshot in the present
28 contribution is the design of a finite element method applied directly to the
29 ill-posed variational data assimilation form. Regularization is then added
30 on the discrete level, using methods from stabilized finite element methods
31 allowing for a detailed analysis using conditional stability estimates.
32
33
34

35 A successful data assimilation method hinges on the existence of some
36 stability properties of the ill-posed problem. Fortunately, it is known that
37 a relatively large class of ill-posed problems has some conditional stability
38 property. Stability estimates give a precise information on the effect of
39 perturbations on the system. In particular, they imply that, if the data
40 are compatible with the PDE, in the sense that there exists a solution in
41 some suitable Sobolev space satisfying both the PDE and the data, then
42 this solution is unique. For the Stokes equation, this unique continuation
43 property was originally proven by Fabre and Lebeau [29]. The analysis of
44 the stability properties of ill-posed problems based on the Navier-Stokes
45 equations is a very active field of research and we refer to the works [36, 4,
46 7, 34, 33, 5, 3] for recent results. Stability estimates for inverse problems
47 classically rely on Carleman inequalities or three-balls inequalities, two tools
48 which are strongly related. The idea of applying Carleman estimates for the
49 stability analysis of inverse problems is introduced in the seminal paper [16]
50 by Bukhgeim and Klibanov.
51
52
53
54
55
56
57
58
59
60

1
2
3
4
5
6
7
8 There appears to be relatively few results in the literature discussing
9 the combined error due to regularization, discretization and perturbations
10 for inverse problems subject to the equations of fluid mechanics. To the
11 best of our knowledge such a combined analysis has only been performed
12 in the recent paper [22], where a nonconforming finite element method was
13 used, together with regularization techniques developed in the context of
14 discontinuous Galerkin methods, to analyze a data assimilation problem for
15 Stokes problem. One of the reasons for this is that there is in general a
16 gap between the stability estimates that can be proven analytically and the
17 stability required to perform a numerical analysis. An approach allowing to
18 bridge this gap was proposed in [19, 20, 21, 23], drawing on earlier ideas for
19 well-posed problems in [12, 13]. This framework combines stabilized finite
20 element methods designed for well-posed problems with variational formu-
21 lations for data assimilation and sharp stability estimates for the continuous
22 problems based on three balls inequalities or Carleman estimates. Recent
23 developments include finite element data assimilation methods with optimal
24 error estimates for the heat equation [25, 24] and design of methods for in-
25 definite or nonsymmetric scalar elliptic problems analyzed using Carleman
26 estimates with explicit dependence on the physical parameters [18, 17].
27
28
29

30
31 In this paper, our aim is to build on these results and use known tech-
32 niques for the approximation of the (well-posed) Navier-Stokes equation in
33 an optimization framework in order to assimilate data with computation.
34 Contrary to the previous work [22], we consider the linearized Navier-Stokes
35 equations and use standard H^1 -conforming, piecewise affine, finite element
36 spaces. The key idea is that the ill-posed continuous problem is not regular-
37 ized. Instead, we discretize the equation and set up a constrained optimiza-
38 tion problem where we minimize the distance between the discrete solution
39 and the measured data. To counter the instabilities in the discrete system,
40 we introduce regularization terms. Taking advantage of the discretize-then-
41 optimize perspective, we get an accuracy which is optimal with respect to
42 the stability of the continuous problem through weakly consistent regular-
43 ization terms. This property is illustrated by the error estimate of Theorem
44 3.1 that is sharp relative to the stability estimate of Corollary 2.1 (which
45 is a consequence of a three balls inequality derived by Lin, Uhlmann and
46 Wang [36]). Moreover, in our framework, the only regularization parameter,
47 up to a constant scaling factor, is the mesh parameter.
48
49

50 We apply this method to an incompressible laminar steady flow in the
51 low Reynolds regime. To be more specific, we are interested in a situation
52 where a known laminar base flow U is available and we consider that a
53
54

1
2
3
4
5
6
7
8 perturbation of the velocity of the base flow has been measured in some
9 subset ω_M of the computational domain Ω . Assuming that the perturbation
10 is small, we then consider the linearized Navier-Stokes equation and our
11 objective is to get quantitative local error estimates for the perturbation in
12 some target subdomain ω_T .
13

14
15 The rest of the paper is organized as follows. In Section 2, we introduce
16 the considered inverse problem and some related stability estimates. In Sec-
17 tion 3, we describe the proposed stabilized finite element approximation of
18 the data assimilation problem and state the local error estimate. The nu-
19 merical analysis of the method is carried out in Section 4. Finally, Section 5
20 presents a series of numerical examples which illustrate the performance of
21 the proposed method. In particular, in Section 5.3, we explore how the
22 present approach can be applied to the estimation of relative pressure in
23 blood flow from MRI velocity measurements.
24
25

26 **2 Presentation of the inverse problem and stabi-** 27 **lity results for the continuous problem** 28 29

30 Let Ω be a bounded open polyhedral domain in \mathbb{R}^d with $d = 2, 3$. We
31 denote by (U, P) a solution of the stationary incompressible Navier-Stokes
32 equations and we consider some perturbation (u, p) of this base flow. It is
33 then known that, if the quadratic term is neglected, the linearized Navier-
34 Stokes equations for (u, p) may be written
35

$$36 \begin{cases} (U \cdot \nabla)u + (u \cdot \nabla)U + \nabla p - \nu \Delta u = f & \text{in } \Omega \\ \nabla \cdot u = 0 & \text{in } \Omega. \end{cases} \quad (1)$$

37
38
39 In what follows, we assume that U belongs to $[W^{1,\infty}(\Omega)]^d$ and that (u, p)
40 satisfies the regularity
41

$$42 (u, p) \in [H^2(\Omega)]^d \times H^1(\Omega).$$

43
44 For this problem, we consider that measurements on u are available in
45 some subdomain $\omega_M \subset \Omega$ having a nonempty interior and our objective is
46 to reconstruct a fluid flow solution of system (1) from these measurements
47 on the velocity.
48

49 Let us now introduce some useful notations. We consider the following
50 spaces
51

$$52 V := [H^1(\Omega)]^d, \quad V_0 := [H_0^1(\Omega)]^d, \quad L_0 := L^2_0(\Omega), \quad \text{and} \quad L := L^2(\Omega)$$

where $L_0^2(\Omega) = \{p \in L^2(\Omega) : \int_{\Omega} p = 0\}$. We also define the norms, for $k = 1$ or d ,

$$\|\cdot\|_L := \|\cdot\|_{[L^2(\Omega)]^k}, \|\cdot\|_V := \|\cdot\|_{[H^1(\Omega)]^k}, \|\cdot\|_{V_0'} := \|\cdot\|_{[H^{-1}(\Omega)]^d}.$$

Let us notice that, in the first two definitions, with some abuse of notation, we use the same notation for $k = 1$ and $k = d$. For any subdomain $\omega \subset \Omega$, we set

$$|v|_{\omega} := \left(\int_{\omega} |v|^2 \right)^{\frac{1}{2}}, \forall v \in L^2(\omega).$$

Besides, we introduce the bilinear forms: for all $(u, v) \in V \times V$

$$a(u, v) := \int_{\Omega} ((U \cdot \nabla)u + (u \cdot \nabla)U) \cdot v + \nu \int_{\Omega} \nabla u : \nabla v, \quad (2)$$

where $H : G := \sum_{i,j=1}^d H_{ij} G_{ij}$ and, for all $(p, v) \in L \times V$

$$b(p, v) := \int_{\Omega} p \nabla \cdot v. \quad (3)$$

The inverse problem we are interested in can be expressed in the following form: $f \in V_0'$ being given, find $(u, p) \in V \times L_0$ such that

$$u = u_M \quad \text{in } \omega_M \quad (4)$$

and

$$a(u, v) - b(p, v) + b(q, u) = \langle f, v \rangle_{V_0', V_0}, \quad \forall (v, q) \in V_0 \times L \quad (5)$$

Here, $u_M \in L^2(\omega_M)$ corresponds to the measurement of the velocity made on ω_M and in what follows we will consider that this measurement corresponds to the exact velocity polluted by a small noise $\delta u \in [L^2(\omega_M)]^d$.

For the analysis of our problem, we also introduce the linearized Navier-Stokes problem with a non-zero velocity divergence

$$\begin{aligned} (U \cdot \nabla)u + (u \cdot \nabla)U - \nu \Delta u + \nabla p &= f & \text{in } \Omega \\ \nabla \cdot u &= g & \text{in } \Omega. \end{aligned} \quad (6)$$

We assume that, if system (6) is completed by homogeneous Dirichlet boundary conditions, then it is well-posed. More precisely, we make the following

assumption:

Assumption A For all $f \in V'_0$ and $g \in L_0$, we assume that system (6) admits a unique weak solution $(u, p) \in V_0 \times L_0$ and that there exists a constant $C_S > 0$ depending only on U and Ω such that

$$\|u\|_V + \|p\|_L \leq C_S(\|f\|_{V'_0} + \|g\|_L). \quad (7)$$

In particular, if $\|\nabla U\|_{[L^\infty(\Omega)]^{d \times d}}$ is small enough, it is straightforward to verify that Assumption A holds according to Lax-Milgram lemma. This assumption of smallness on ∇U however is a sufficient condition and there are reasons to believe that the assumption holds in more general cases.

In the homogeneous case (which corresponds to $f = 0$ in (1) or to $f = 0$ and $g = 0$ in (6)), a solution (u, p) satisfies a three-balls inequality which only involves the L^2 norm of the velocity. This three-balls inequality result is stated in [36] (with their notations, A corresponds to U and B to ∇U) and we recall it here. We emphasise the fact that, in this theorem and in its corollary, no boundary conditions are prescribed.

Theorem 2.1 (*Three-balls inequality*) *There exists $\tilde{R} \in (0, 1)$ such that for all $0 < R_1 < R_2 < R_3 \leq R_0$ and $x_0 \in \Omega$ satisfying $R_1/R_3 < R_2/R_3 < \tilde{R}$ and $B_{R_0}(x_0) \subset \Omega$, we have*

$$\int_{B_{R_2}(x_0)} |u|^2 \leq C \left(\int_{B_{R_3}(x_0)} |u|^2 \right)^{1-\tau} \left(\int_{B_{R_1}(x_0)} |u|^2 \right)^\tau \quad (8)$$

for $(u, p) \in [H^1(B_{R_0}(x_0))]^d \times H^1(B_{R_0}(x_0))$, solution of (1) with $f = 0$ in $B_{R_0}(x_0)$. In this inequality, C depends on R_2/R_3 and $0 < \tau < 1$ depends on R_1/R_3 , R_2/R_3 and d .

This theorem combined with Assumption A implies a local stability inequality in the non-homogeneous case given by system (6). This stability property will be capital in the convergence study of the numerical method and is given by the following statement:

Corollary 2.1 (*Conditional stability for the linearized Navier-Stokes problem*) *Let $f \in V'_0$ and $g \in L_0$ be given. For all $\omega_T \subset \subset \Omega$, there exist $C > 0$ and $0 < \tau < 1$ such that*

$$|u|_{\omega_T} \leq C(\|f\|_{V'_0} + \|g\|_L + \|u\|_L)^{1-\tau} (\|f\|_{V'_0} + \|g\|_L + |u|_{\omega_M})^\tau \quad (9)$$

for all $(u, p) \in [H^1(\Omega)]^d \times H^1(\Omega)$ solution of (6).

The proof of Corollary 2.1 is given in Appendix A. In a classical way for ill-posed problems [1], Corollary 2.1 gives a conditional stability result in the sense that, to be useful, this estimate has to be accompanied with an a priori bound on the solution on the global domain (due to the presence of $\|u\|_L$ in the right hand side). Let us notice that Corollary 2.1 implies in particular the uniqueness of a solution (u, p) in $[H^1(\Omega)]^d \times H^1(\Omega)$ for problem (4)-(5), up to a constant for p . Moreover, in inequality (9), the exponent τ depends on the dimension d , the size of the measure domain ω_M and the distance between the target domain ω_T and the boundary of the computational domain Ω .

Remark 2.1 *Herein, we only consider error estimates for local L^2 -norms, but errors in local H^1 -norms of velocity together with L^2 -norms of pressure are also possible to analyse using three balls inequalities derived in [7], provided measurements of both velocities and pressures are available in ω_M .*

In what follows, we assume that $f \in L^2(\Omega)$ and we introduce the operator A defined on $(V \times L_0) \times (V_0 \times L)$ by

$$A[(u, p), (v, q)] := a(u, v) - b(p, v) + b(q, u) \quad (10)$$

where a and b are respectively defined by (2) and (3). Thus, we look for $(u, p) \in V \times L_0$ such that

$$A[(u, p), (v, q)] = (f, v)_{L^2(\Omega)}, \quad \forall (v, q) \in V_0 \times L \quad (11)$$

and (4) holds.

3 Stabilized finite element approximation and error estimate

In this section, we first introduce a discretization of problem (11) using a standard finite element method. Then, the discrete inverse problem is reformulated as a constrained minimization problem in the discrete space where the regularization of the cost functional is achieved through stabilization terms. At last, the estimation of the error between the exact continuous solution and the discrete solution of our minimization problem is stated in Theorem 3.1 which corresponds to our main theoretical result.

On the domain Ω , we consider a family $\{\mathcal{T}_h\}_h$ of shape regular, conforming, quasi-uniform meshes consisting of shape regular simplices K . This

family is indexed by h defined as the maximum over the diameters h_K of elements in the mesh. For a fixed $h > 0$, we denote by \mathcal{F}_i the set of interior faces of the mesh \mathcal{T}_h .

We will also use the notion of jump over a face F shared by the elements K and K' (which means that $F = \bar{K} \cap \bar{K}'$) defined as follows: if ζ is a scalar,

$$[[\zeta]]_F = \zeta|_K - \zeta|_{K'}$$

and, if ζ is a vector,

$$[[\zeta]]_F = \zeta|_K \cdot n_K + \zeta|_{K'} \cdot n_{K'}$$

where n_K denotes the outward pointing normal of the element K .

We denote by X_h the standard H^1 -conforming finite element space of piecewise affine functions defined on \mathcal{T}_h and we introduce

$$V_h := [X_h]^d, \quad W_h := V_h \cap V_0, \quad Q_h := X_h \text{ and } Q_h^0 := X_h \cap L_0.$$

We may then write the finite element approximation of (11): find $(u_h, p_h) \in V_h \times Q_h^0$ such that

$$A[(u_h, p_h), (v_h, q_h)] = (f, v_h)_{L^2(\Omega)} \quad (12)$$

for all $(v_h, q_h) \in W_h \times Q_h$.

To take into account the measurements on ω_M given by (4), we introduce the measurement bilinear form

$$m(u, v) = \gamma_M \int_{\omega_M} uv,$$

where $\gamma_M > 0$ will correspond to a free parameter representing the relative confidence in the measurements. The objective is then to minimize the functional

$$\frac{1}{2} m(u_M - u_h, u_M - u_h)$$

under the constraint that (u_h, p_h) satisfies (12). However, the discrete Lagrangian associated to this problem leads to an optimality system which is ill-posed. To regularize it, we introduce stabilization operators that will convexify the problem with respect to the direct variables u_h, p_h and the

adjoint variables z_h, w_h . We define $s_u : V_h \times V_h \mapsto \mathbb{R}$, $s_u^* : W_h \times W_h \mapsto \mathbb{R}$,
 $s_p : Q_h^0 \times Q_h^0 \mapsto \mathbb{R}$ and $s_p^* : Q_h \times Q_h \mapsto \mathbb{R}$ by

$$s_u(u_h, v_h) := \gamma_u \sum_{F \in \mathcal{F}_i} \int_F h_F [[\nabla u_h]] [[\nabla v_h]] + \gamma_{div} \int_{\Omega} (\nabla \cdot u_h)(\nabla \cdot v_h),$$

$$s_p(p_h, q_h) := \gamma_p \int_{\Omega} h^2 \nabla p_h \cdot \nabla q_h$$

and

$$s_u^*(z_h, w_h) := \gamma_u^* \int_{\Omega} \nabla z_h : \nabla w_h, \quad s_p^*(y_h, x_h) := \gamma_p^* \int_{\Omega} y_h x_h,$$

where $\gamma_u, \gamma_p, \gamma_u^*$ and γ_p^* are positive user-defined parameters. Let us make some comments on these stabilization terms. The stabilization of the direct velocity acts on fluctuations of the discrete solution through a penalty on the jump of the solution gradient over element faces and has no equivalent on the continuous level. On the other hand, for the forward equation, the pressure stabilization s_p coincides with a standard H^1 -Tikhonov regularization (let us notice that this stabilization term also appears the Brezzi-Pitkäranta method [14]). Since the exact solution of the adjoint equation is zero, consistency is ensured also for Tikhonov type regularization. For a more general discussion of the possible stabilization operators, we refer to [19, 21].

For compactness, we introduce the primal and dual stabilizers: for all $(u_h, p_h), (v_h, q_h) \in V_h \times Q_h^0$

$$S[(u_h, p_h), (v_h, q_h)] = s_u(u_h, v_h) + s_p(p_h, q_h)$$

and, for all $(z_h, y_h), (w_h, x_h) \in W_h \times Q_h$

$$S^*[(z_h, y_h), (w_h, x_h)] = s_u^*(z_h, w_h) + s_p^*(y_h, x_h).$$

We may then write the discrete Lagrangian

$$\mathcal{L} : (V_h \times Q_h^0) \times (W_h \times Q_h) \mapsto \mathbb{R}$$

that will form the basis of our method as: for all $(u_h, p_h) \in (V_h \times Q_h^0)$ and $(z_h, y_h) \in (W_h \times Q_h)$

$$\begin{aligned} \mathcal{L}[(u_h, p_h), (z_h, y_h)] &:= \frac{1}{2} m(u_M - u_h, u_M - u_h) + A[(u_h, p_h), (z_h, y_h)] \\ &\quad - (f, z_h)_{L^2(\Omega)} + \frac{1}{2} S[(u_h, p_h), (u_h, p_h)] - \frac{1}{2} S^*[(z_h, y_h), (z_h, y_h)]. \end{aligned} \quad (13)$$

If we differentiate with respect to (u_h, p_h) and (z_h, y_h) , we get the following optimality system: find $(u_h, p_h) \in V_h \times Q_h^0$ and $(z_h, y_h) \in W_h \times Q_h$ such that

$$\begin{aligned} A[(u_h, p_h), (w_h, x_h)] - S^*[(z_h, y_h), (w_h, x_h)] &= (f, w_h)_{L^2(\Omega)} \\ A[(v_h, q_h), (z_h, y_h)] + S[(u_h, p_h), (v_h, q_h)] + m(u_h, v_h) &= m(u_M, v_h) \end{aligned} \quad (14)$$

for all $(v_h, q_h) \in V_h \times Q_h^0$ and all $(w_h, x_h) \in W_h \times Q_h$.

Let us prove that this discrete problem is well-posed. To do so, we recall a Poincaré inequality from [23, Lemma 2] that will be crucial to get the stability of the method:

$$h\|v_h\|_V \lesssim (s_u(v_h, v_h) + \gamma_M |v_h|_{\omega_M}^2)^{\frac{1}{2}}, \quad \forall v_h \in V_h. \quad (15)$$

If we take in the variational formulation (14) the test functions $w_h = -z_h$, $x_h = -y_h$ and $v_h = u_h$, $q_h = p_h$ we see that, for any solution $(u_h, p_h) \in V_h \times Q_h^0$, $(z_h, y_h) \in W_h \times Q_h$, there holds

$$S[(u_h, p_h), (u_h, p_h)] + S^*[(z_h, y_h), (z_h, y_h)] + \gamma_M |u_h|_{\omega_M}^2 = -(f, z_h)_L + m(u_M, u_h). \quad (16)$$

Then, according to (15), the left hand side in equation (16) is the square of a norm in $(V_h \times Q_h^0) \times (W_h \times Q_h)$ and, according to Babuska-Necas-Brezzi theorem (see [28]), we conclude that the square linear system defined by (14) admits a unique solution for all $h > 0$.

The following theorem is the main theoretical result of the paper and states an error estimate for this method.

Theorem 3.1 *Let $f \in L^2(\Omega)$ and $\delta u \in L^2(\omega_M)$ be given. We assume that (u, p) solution of (11) belongs to $[H^2(\Omega)]^d \times H^1(\Omega)$ and we consider $(u_h, p_h) \in V_h \times Q_h^0$, $(z_h, y_h) \in W_h \times Q_h$ the discrete solution of (14) where $u_M := u|_{\omega_M} + \delta u$. Then, for all $\omega_T \subset\subset \Omega$, there exists $\tau \in (0, 1)$ such that*

$$|u - u_h|_{\omega_T} \leq Ch^\tau (\|u\|_{[H^2(\Omega)]^d} + \|p\|_{H^1(\Omega)} + h^{-1} |\delta u|_{\omega_M}) + h\|f\|_L. \quad (17)$$

The constant C depends on the geometry of ω_M and ω_T and on $\|U\|_{[W^{1,\infty}(\Omega)]^{d \times d}}$.

The proof of this result will strongly rely on the conditional stability estimate for the continuous problem given by Corollary 2.1 and the convergence of the residual quantities given by Lemma 4.3.

According to this theorem, we get that, if the measurement noise δu is equal to 0, the error $u - u_h$ converges to 0 when h tends to 0 on any subset $\omega_T \subset\subset \Omega$. Moreover, the convergence order τ corresponds to the Hölder coefficient of the continuous stability estimate (9). On the other hand, in the

case of perturbed data, we notice that the accuracy of the error is limited and inequality (17) shows that the mesh size has to balance the error due to the discretization and the error due to the noise.

Remark 3.1 *For simplicity, we restrict the discussion to piecewise affine continuous approximation spaces, but the arguments can be extended to higher order finite element spaces, with the expected improvement of convergence order, following the ideas of [21]. It should however be noted that the system matrix becomes increasingly ill-posed as the polynomial order increases and the computation becomes more sensitive to noise in the measured data, so the practical interest in using high order approximation spaces remains to be proven.*

4 Stability and error analysis

In this section, we will present and prove several technical results and end with the proof of Theorem 3.1.

Let us first notice that formulation (14) is weakly consistent in the sense that we have a modified Galerkin orthogonality relation with respect to the scalar product associated to A :

Lemma 4.1 *(Consistency) Let (u, p) satisfy (1) and (u_h, p_h) be a solution of (14). Then there holds*

$$A[(u - u_h, p - p_h), (w_h, x_h)] = -S^*[(z_h, y_h), (w_h, x_h)] \quad (18)$$

for all $(w_h, x_h) \in W_h \times Q_h$.

Proof: The result is immediate by taking the difference between (11) and the first equation of (14). \square

In the analysis below, we will use the following classical inverse and trace inequalities:

- Inverse inequality (see [27, Section 1.4.3]),

$$|v|_{H^1(K)} \lesssim h_K^{-1} \|v\|_{L^2(K)} \quad \forall v \in \mathbb{P}_1(K). \quad (19)$$

Here $\mathbb{P}_1(K)$ denotes the set of polynomials of degree less than or equal to 1 on the simplex K .

- Trace inequalities (see [27, Section 1.4.3]),

$$\|v\|_{L^2(\partial K)} \leq C \left(h_K^{-\frac{1}{2}} \|v\|_{L^2(K)} + h_K^{\frac{1}{2}} \|v\|_{H^1(K)} \right) \quad \forall v \in H^1(K). \quad (20)$$

At last, by combining (20) and (19)

$$\|v\|_{L^2(\partial K)} \leq Ch_K^{-\frac{1}{2}} \|v\|_{L^2(K)} \quad \forall v \in \mathbb{P}_1(K). \quad (21)$$

Let us now define the semi-norms associated to the stabilization operators defined on $([H^2(\Omega)]^d + V_h) \times (H^1(\Omega) + Q_h)$

$$\| |(v, q)| \| = h \|v\|_V + S[(v, q), (v, q)]^{\frac{1}{2}}, \quad \| |(v, q)| \|_* = S^*[(v, q), (v, q)]^{\frac{1}{2}}.$$

We also introduce the norm

$$\|(v, q)\|_{\#} := \|v\|_V + \|q\|_L.$$

Let $i_h : L^2(\Omega) \mapsto X_h$ be the Scott-Zhang interpolant. We refer to [28] for the following results: for $t = 1, 2$, we have, for all $u \in H^t(\Omega)$

$$\|u - i_h u\|_{\Omega} + h \|\nabla(u - i_h u)\|_{\Omega} + h^{\frac{1}{2}} \left(\sum_K \|u - i_h u\|_{\partial K}^2 \right)^{1/2} \leq Ch^t |u|_{H^t(\Omega)} \quad (22)$$

and for all $u \in H^2(\Omega)$

$$\left(\sum_{F \in \mathcal{F}_h} \|\nabla(u - i_h u) \cdot n\|_F^2 \right)^{1/2} \leq h^{\frac{1}{2}} |u|_{H^2(\Omega)}.$$

Using the componentwise extension of i_h to vectorial functions, we deduce the approximation bounds: $\forall (v, q) \in [H^2(\Omega)]^d \times H^1(\Omega)$

$$\| |(v - i_h v, q - i_h q)| \| + \|(v - i_h v, q - i_h q)\|_{\#} \lesssim h(\|v\|_{H^2(\Omega)} + \|q\|_{H^1(\Omega)}). \quad (23)$$

The following continuity results for the bilinear form A motivate the definition of the triple norms.

Lemma 4.2 (Continuity) *For all $\varsigma \in V_h + [H^2(\Omega)]^d$ and $\varpi \in Q_h + H^1(\Omega)$ there holds*

$$A[(\varsigma, \varpi), (v_h, q_h)] \lesssim \|(\varsigma, \varpi)\|_{\#} \| |(v_h, q_h)| \|_*, \quad \forall (v_h, q_h) \in W_h \times Q_h \quad (24)$$

and, for all $(v_h, q_h) \in V_h \times Q_h^0$, for all $w \in [H_0^1(\Omega)]^d$ and $y \in L^2(\Omega)$

$$A[(v_h, q_h), (w - w_h, y - y_h)] \leq \| |(v_h, q_h)| \| (\|w\|_V + \|y\|_L) \quad (25)$$

where $(w_h, y_h) = (i_h w, i_h y)$.

Proof: The proof of (24) directly comes from the Cauchy-Schwarz inequality applied termwise in the definition (10) of A . For the second inequality (25), we set $\tilde{w} = w - w_h$ and $\tilde{y} = y - y_h$ and notice that

$$A[(v_h, q_h), (\tilde{w}, \tilde{y})] := a(v_h, \tilde{w}) - b(q_h, \tilde{w}) + b(\tilde{y}, v_h). \quad (26)$$

For the first term in the right hand side, an integration by parts in the viscous term gives, observing that $\tilde{w}|_{\partial\Omega} = 0$,

$$a(v_h, \tilde{w}) \lesssim \|U\|_{[W^{1,\infty}(\Omega)]^d} \|h v_h\|_V \|h^{-1} \tilde{w}\|_L + \frac{1}{2} \sum_{F \in \mathcal{F}_i} \int_F [[\nabla v_h \cdot n]] \cdot \tilde{w} \, ds.$$

Using Cauchy-Schwarz inequality with the right scaling in h , we get

$$a(v_h, \tilde{w}) \lesssim \|U\|_{[W^{1,\infty}(\Omega)]^d} \|h v_h\|_V \|h^{-1} \tilde{w}\|_L + \sum_{F \in \mathcal{F}_i} \|h^{\frac{1}{2}} [[\nabla v_h]]\|_F \|h^{-\frac{1}{2}} \tilde{w}\|_F.$$

Applying the trace inequality (20), we notice that

$$\|h^{-1} \tilde{w}\|_K + \|h^{-\frac{1}{2}} \tilde{w}\|_{\partial K} \lesssim h^{-1} \|\tilde{w}\|_K + \|\nabla \tilde{w}\|_K.$$

Then, if we take the square, sum over K and use the H^1 -stability inequality of i_h (22) for $t = 1$, this inequality becomes

$$\|h^{-1} \tilde{w}\|_L + \left(\sum_{F \in \mathcal{F}_i} \|h^{-\frac{1}{2}} \tilde{w}\|_F^2 \right)^{1/2} \lesssim \|w\|_V.$$

As a consequence

$$a(v_h, \tilde{w}) \lesssim |(v_h, 0)| \|w\|_V.$$

Similarly, for the second term in (26), an integration by parts gives

$$|b(q_h, \tilde{w})| \leq \|h \nabla q_h\|_L \|h^{-1} \tilde{w}\|_L \lesssim |(0, q_h)| \|w\|_V.$$

Finally, the bound for the third term in (26) is immediate by the Cauchy-Schwarz inequality and the L^2 -stability of i_h

$$|b(\tilde{y}, v_h)| \leq \|\nabla \cdot v_h\|_L \|\tilde{y}\|_L \lesssim |(v_h, 0)| \|y\|_L.$$

Gathering these results, we get (25). \square

Remark 4.1 *The augmented Lagrangian stabilization on the divergence in the operator s_u is used in the proof of Lemma 4.2 to bound in a direct way the third term in (26) but it is not strictly necessary. Indeed, if y_h is chosen as the L^2 -projection of y we see that for all $x_h \in Q_h$,*

$$b(\tilde{y}, v_h) = (\tilde{y}, \nabla \cdot v_h - x_h)_L$$

and recalling that

$$\inf_{x_h \in Q_h} \|\nabla \cdot v_h - x_h\|_L \lesssim \left(\sum_{F \in \mathcal{F}_i} h_F \|\llbracket \nabla \cdot v_h \rrbracket\|_F^2 \right)^{\frac{1}{2}}$$

we conclude that

$$b(\tilde{y}, v_h) \lesssim \|y\|_L \left(\sum_{F \in \mathcal{F}_i} h_F \|\llbracket \nabla v_h \rrbracket\|_F^2 \right)^{\frac{1}{2}}.$$

Hence, the stabilization of the gradient jump is sufficient to bound this term. In practice however, it can be useful to add the stabilization term on the divergence since it allows to get a stronger coercivity estimate.

The above lemma asserts that some residual converges with optimal order if the exact solution is smooth enough.

Lemma 4.3 *We assume that the solution (u, p) of (11) belongs to $[H^2(\Omega)]^d \times H^1(\Omega)$ and we consider $(u_h, p_h) \in V_h \times Q_h^0$, $(z_h, y_h) \in W_h \times Q_h$ the discrete solution of (14). Then there holds*

$$\begin{aligned} & \|\llbracket (u - u_h, p - p_h) \rrbracket\| + \|\llbracket (z_h, y_h) \rrbracket\|_* + \gamma_M^{1/2} |u - u_h|_{\omega_M} \\ & \leq Ch(\|u\|_{[H^2(\Omega)]^d} + \|p\|_{H^1(\Omega)}) + \gamma_M^{1/2} |\delta u|_{\omega_M}. \end{aligned}$$

Proof: We introduce the discrete errors $\xi_h = i_h u - u_h$, $\eta_h = i_h p - p_h$. By this way, $(u - u_h, p - p_h) = (u - i_h u, p - i_h p) + (\xi_h, \eta_h)$. First we observe that

$$\begin{aligned} & \|\llbracket (u - u_h, p - p_h) \rrbracket\| + \gamma_M^{1/2} |u - u_h|_{\omega_M} \\ & \leq \|\llbracket (u - i_h u, p - i_h p) \rrbracket\| + \gamma_M^{1/2} |u - i_h u|_{\omega_M} + \|\llbracket (\xi_h, \eta_h) \rrbracket\| + \gamma_M^{1/2} |\xi_h|_{\omega_M}. \end{aligned}$$

Using inequalities (23) and (22) for $t = 1$, we can directly bound the first two terms in the right hand side. For the last two terms, according to inequality (15), we have

$$\|(\xi_h, \eta_h)\|_M^2 + \gamma_M |\xi_h|_{\omega_M}^2 \lesssim S[(\xi_h, \eta_h), (\xi_h, \eta_h)] + \gamma_M |\xi_h|_{\omega_M}^2.$$

To estimate the right hand side, we notice that, using the second equation of (14) with $(v_h, q_h) = (\xi_h, \eta_h)$

$$\begin{aligned} S[(\xi_h, \eta_h), (\xi_h, \eta_h)] + \gamma_M |\xi_h|_{\omega_M}^2 - A[(\xi_h, \eta_h), (z_h, y_h)] = \\ S[(i_h u, i_h p), (\xi_h, \eta_h)] + m(i_h u - u, \xi_h) - m(\delta u, \xi_h). \end{aligned}$$

Next, according to (18) with $(w_h, x_h) = (z_h, y_h)$, we have

$$\|(z_h, y_h)\|_*^2 + A[(\xi_h, \eta_h), (z_h, y_h)] = A[(i_h u - u, i_h p - p), (z_h, y_h)].$$

Thus, adding these two equalities, we get

$$\begin{aligned} S[(\xi_h, \eta_h), (\xi_h, \eta_h)] + |\xi_h|_{\omega_M}^2 + \|(z_h, y_h)\|_*^2 = \underbrace{A[(i_h u - u, i_h p - p), (z_h, y_h)]}_I \\ + \underbrace{S[(i_h u, i_h p), (\xi_h, \eta_h)]}_{II} + \underbrace{m(i_h u - u, \xi_h) - m(\delta u, \xi_h)}_{III}. \end{aligned}$$

We bound the terms I – III term by term. By Lemma 4.2 and the approximation bound (23), we have for term I

$$I \lesssim \|(i_h u - u, i_h p - p)\|_{\#} \|(z_h, y_h)\|_* \lesssim h(\|u\|_{[H^2(\Omega)]^d} + \|p\|_{H^1(\Omega)}) \|(z_h, y_h)\|_*.$$

For term II , we have

$$S[(i_h u, i_h p), (\xi_h, \eta_h)] = S[(i_h u - u, 0), (\xi_h, \eta_h)] + \gamma_p \int_{\Omega} h^2 \nabla i_h p \cdot \nabla \eta_h.$$

Thus, using (23) with $(v, q) = (u, p)$ for the first term and the H^1 -stability of i_h for the second term, we get

$$II \lesssim h(\|u\|_{[H^2(\Omega)]^d} + \|p\|_{H^1(\Omega)}) \|(\xi_h, \eta_h)\|_M.$$

For term III , according to (22) with $t = 2$, we have

$$\begin{aligned} III &\leq \gamma_M (|i_h u - u|_{\omega_M} + |\delta u|_{\omega_M}) |\xi_h|_{\omega_M} \\ &\leq (Ch^2 \|u\|_{H^2(\Omega)} + \gamma_M^{1/2} |\delta u|_{\omega_M}) \gamma_M^{1/2} |\xi_h|_{\omega_M}. \end{aligned}$$

Thus, collecting the above bounds, we get

$$\begin{aligned} & \|\|(\xi_h, \eta_h)\|\|^2 + \|\|(z_h, y_h)\|\|_*^2 + \gamma_M |\xi_h|_{\omega_M}^2 \\ & \lesssim (h(\|u\|_{[H^2(\Omega)]^d} + \|p\|_{H^1(\Omega)}) + \gamma_M^{1/2} |\delta u|_{\omega_M}) (\|\|(\xi_h, \eta_h)\|\|^2 + \gamma_M |\xi_h|_{\omega_M}^2 + \|\|(z_h, y_h)\|\|_*^2)^{\frac{1}{2}} \end{aligned}$$

and we conclude by dividing by $(\|\|(\xi_h, \eta_h)\|\|^2 + \gamma_M^{1/2} |\xi_h|_{\omega_M}^2 + \|\|(z_h, y_h)\|\|_*^2)^{\frac{1}{2}}$.

□

We then deduce from the previous lemma a priori bounds on the finite element solution.

Corollary 4.1 *Under the same assumptions as for Lemma 4.3, there holds*

$$\|\|(u_h, p_h)\|\| \lesssim h(\|u\|_{[H^2(\Omega)]^d} + \|p\|_{H^1(\Omega)}) + \gamma_M^{1/2} |\delta u|_{\omega_M} \quad (27)$$

and

$$\|u_h\|_V + \|p_h\|_{H^1(\Omega)} \lesssim \|u\|_{[H^2(\Omega)]^d} + \|p\|_{H^1(\Omega)} + h^{-1} \gamma_M^{1/2} |\delta u|_{\omega_M}. \quad (28)$$

Proof: In an evident way, we have

$$\|\|(u_h, p_h)\|\| \leq \|\|(u_h - u, p_h - p)\|\| + \|\|(u, p)\|\|.$$

Thus, according to Lemma 4.3 and the fact that $\|\|(u, p)\|\| = h\|u\|_V + s_p(p, p)^{\frac{1}{2}}$, we get (27). Moreover, by definition of $\|\| \cdot \|\|$, we have

$$\|u_h\|_V + \|p_h\|_{H^1(\Omega)} \lesssim h^{-1} \|\|(u_h, p_h)\|\|.$$

Thus inequality (27) directly implies (28). □

We are now ready to prove our main result stated in Theorem 3.1.

Proof of Theorem 3.1: Let us first introduce the weak formulation of the problem satisfied by $(\xi, \eta) := (u - u_h, p - p_h)$. By equation (11), we have for all $w \in V_0$ and $q \in L$,

$$A[(\xi, \eta), (w, q)] = (f, w)_{L^2(\Omega)} - A[(u_h, p_h), (w, q)]$$

We introduce, u_h and p_h being fixed, the linear forms r_f and r_g on V_0 and L respectively defined by: for all $w \in V_0$ and $q \in L$,

$$\langle r_f, w \rangle_{V_0', V_0} + (r_g, q)_L := (f, w)_{L^2(\Omega)} - A[(u_h, p_h), (w, q)].$$

It follows that (ξ, η) is solution of (6) with the functions f and g in the right hand sides replaced respectively by r_f and r_g . Applying now Corollary 2.1, we directly get

$$|\xi|_{\omega_T} \leq C(\|r_f\|_{V_0'} + \|r_g\|_L + \|\xi\|_L)^{1-\tau} (\|r_f\|_{V_0'} + \|r_g\|_L + |\xi|_{\omega_M})^\tau. \quad (29)$$

Using the first equation of (14), we can write the residuals: for all $(w_h, q_h) \in W_h \times Q_h$

$$\begin{aligned} & \langle r_f, w \rangle_{V'_0, V_0} + (r_g, q)_L \\ &= (f, w - w_h)_{L^2(\Omega)} - A[(u_h, p_h), (w - w_h, q - q_h)] - S^*[(z_h, y_h), (w_h, q_h)]. \end{aligned}$$

We take $w_h = i_h w$ and $q_h = i_h q$ in this equality. For the first term, according to (22) for $t = 1$, we have

$$|(f, w - w_h)_{L^2(\Omega)}| \leq h \|f\|_L \|w\|_V.$$

The second term can be bounded by using the relations (25) and (27). For the last term, we have, according to Lemma 4.3

$$\begin{aligned} |S^*[(z_h, y_h), (w_h, q_h)]| &\leq \| (z_h, y_h) \|_* \| (w_h, q_h) \|_{\#} \\ &\lesssim (hC(u, p) + |\delta u|_{\omega_M}) \| (w, q) \|_{\#} \end{aligned}$$

where

$$C(u, p) := \|u\|_{[H^2(\Omega)]^d} + \|p\|_{H^1(\Omega)}.$$

We thus get

$$\langle r_f, w \rangle_{V'_0, V_0} + (r_g, q)_L \lesssim (hC(u, p) + |\delta u|_{\omega_M} + h\|f\|_L + \|(\xi, \eta)\|) \| (w, q) \|_{\#}.$$

Since this bound holds for all $w \in V_0$ and $q \in L$, we conclude that

$$\|r_f\|_{V'_0} + \|r_g\|_L \lesssim hC(u, p) + |\delta u|_{\omega_M} + h\|f\|_L + \|(\xi, \eta)\|.$$

Thus, we can bound the terms in the right hand side of (29) in the following way:

$$\|r_f\|_{V'_0} + \|r_g\|_L + \|\xi\|_L \lesssim C(u, p) + h\|f\|_L + h^{-1}|\delta u|_{\omega_M}$$

according to inequalities (27) and (28) and

$$\|r_f\|_{V'_0} + \|r_g\|_L + \|\xi\|_{\omega_M} \lesssim hC(u, p) + h\|f\|_L + |\delta u|_{\omega_M}$$

according to Lemma 4.3.

Using these two bounds in (29), we conclude that

$$\begin{aligned} |\xi|_{\omega_T} &\lesssim (C(u, p) + h^{-1}|\delta u|_{\omega_M})^{1-\tau} (hC(u, p) + |\delta u|_{\omega_M})^{\tau} + h\|f\|_L \\ &\lesssim h^{\tau} (C(u, p) + h^{-1}|\delta u|_{\omega_M}) + h\|f\|_L, \end{aligned}$$

which completes the proof of Theorem 3.1.

5 Numerical simulations

In this section, we apply the method introduced in Section 3 in different two-dimensional different numerical examples. The free parameters in (14) are set to

$$\gamma_u = \gamma_{div} = \gamma_p = \gamma_u^* = \gamma_p^* = 10^{-1}, \quad \gamma_M = 1000,$$

in all the numerical examples. The numerical computations have been performed with FreeFEM++ (see [31]).

5.1 Convergence study: Stokes example

In order to illustrate the convergence behavior of the method introduced in Section 3, we take up the test case presented in [22] for the Stokes system. In the unit square $\Omega = (0, 1)^2$, we consider the velocity and pressure fields

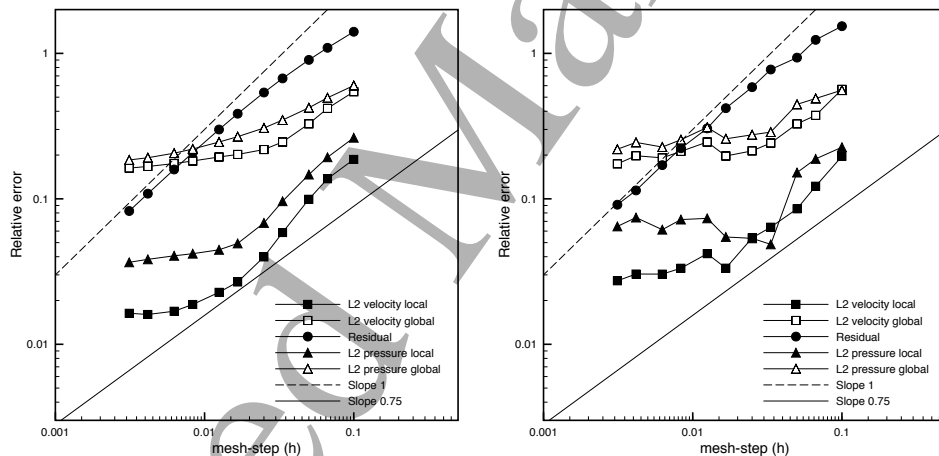


Figure 1: Relative errors against mesh size for the Stokes problem. Left: without noise. Right: with 10% noise.

given by

$$u(x, y) = (20xy^3, 5x^4 - 5y^4), \quad p(x, y) = 60x^2y - 20y^3 - 5.$$

It is straightforward to verify that (u, p) is a solution to the homogeneous Stokes problem with $\nu = 1$, which corresponds to system (1) with $U = 0$ and $f = 0$. We hence consider the formulation (14) with $U = 0$ and $f = 0$. The measurement and target subdomains are defined by

$$\omega_M := (0.75, 1) \times (0.25, 0.75), \quad \omega_T := (0.25, 1) \times (0.25, 0.75).$$

First, we perform the computation with unperturbed data. In Figure 1 (left), we report the velocity and pressure errors both in the global L^2 -norm and the local L^2 -norm in the subdomain ω_Γ . We also provide the convergence history of the residual quantity for the velocity stabilization:

$$\left(\sum_{F \in \mathcal{F}_i} \gamma_u \int_F \|h^{\frac{1}{2}} [\nabla u_h]\|_{\mathcal{F}}^2 \right)^{\frac{1}{2}}.$$

The observed global asymptotic behaviors of the local velocity error (filled squares) and residual (filled circles) are in agreement with the convergence rates obtained in Theorem 3.1 and Corollary 4.1 with $|\delta u|_{\omega_M} = 0$. It should be noted that, for the finest grids, the local velocity error tends to stagnate or increase, which can be related either to the impact of the rounding-off errors or to ill-conditioning issues of the system matrix, so that $|\delta u|_{\omega_M} > 0$. The other error quantities, global velocity error (empty squares) and local and global pressure errors (filled and empty triangles, respectively) show a convergent behavior which also tends to stagnate for the smallest values of h . Figure 1 (right) presents the convergence history of the same quantities with a 10% Gaussian noise. The impact of the noise is clearly visible. In particular, it is worth noting that the convergence history of the local and global velocity and pressure errors is not monotone anymore and the residual loses first-order convergence rate. This is also in agreement with Theorem 3.1 and Corollary 4.1 with $|\delta u|_{\omega_M} > 0$.

5.2 Convergence study: linearized Navier-Stokes example

In this subsection, we will use Taylor-Green vortices to construct exact solutions of (1). Let us first introduce a flow of size $R\pi$ described by a Taylor-Green vortex:

$$u_R(x, y) := \begin{pmatrix} -\sin(x/R) \cos(y/R) \exp(-2\nu t/R^2) \\ \cos(x/R) \sin(y/R) \exp(-2\nu t/R^2) \end{pmatrix},$$

$$p_R(x, y) := \frac{1}{4}(\cos(2x/R) + \cos(2y/R)) \exp(-4\nu t/R^2).$$

For any $R > 0$, we can check that (u_R, p_R) is solution of the unsteady Navier-Stokes equations. In our numerical example, we take $\Omega = (0, 2\pi)^2$ and consider the following system which admits $(u_{\frac{1}{2}}, p_{\frac{1}{2}})$ as solution:

$$\begin{cases} (u_1 \cdot \nabla)u + (u \cdot \nabla)u_1 - \nu \Delta u + \nabla p = f & \text{in } \Omega \\ \nabla \cdot u = 0 & \text{in } \Omega \end{cases}$$

where f is given by

$$f = -(u_{\frac{1}{2}} \cdot \nabla)u_{\frac{1}{2}} + (u_1 \cdot \nabla)u_{\frac{1}{2}} + (u_{\frac{1}{2}} \cdot \nabla)u_1 - \partial_t u_{\frac{1}{2}}.$$

Thus, f and u_1 being given, we can use the method presented in Section 3 to reconstruct u and p from measurements on ω_M . The measurement and target subdomains are defined by

$$\begin{aligned} \omega_M &:= (0, \pi/2) \times (\pi/2, 3\pi/2) \cup (3\pi/2, 2\pi) \times (\pi/2, 3\pi/2), \\ \omega_T &:= (\pi/2, 2\pi) \times (\pi/2, 3\pi/2). \end{aligned}$$

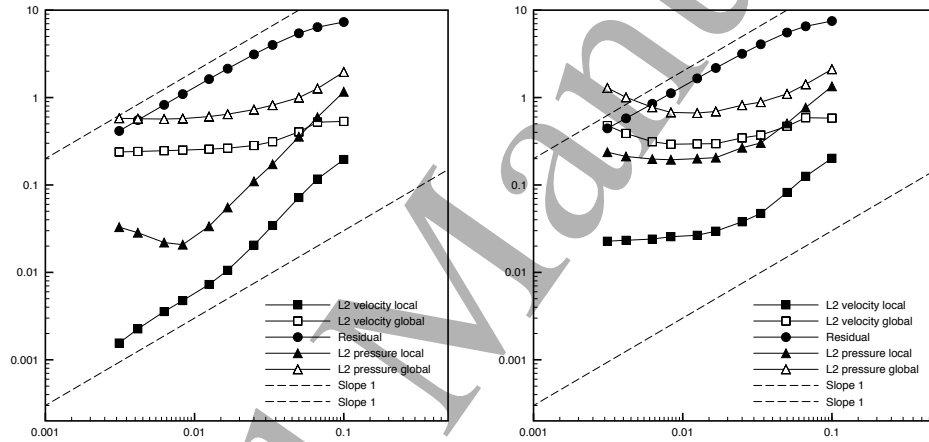


Figure 2: Relative errors against mesh size for the linearized Navier-Stokes problem. Left: without noise. Right: with 10% noise.

As in the previous case, we have performed numerical tests for unperturbed data and for data perturbed with a 10% noise and we have studied the convergence of the method. The obtained results are illustrated in Figure 2. The convergence curves present similarities with the ones obtained in Figure 1. We can all the same notice that, for unperturbed data, the evolution of the local velocity error is more satisfactory: it is close to the linear behavior and the error reaches much smaller values.

5.3 Application: relative blood pressure estimation from velocity measurements

To evaluate the risks related to a constriction (also called stenosis) in a blood vessel, the relative pressure difference (RPD) is a standard clinical

bio-marker. Direct blood pressure measurements can however only be obtained through invasive procedures like catheterization. Non-invasive measurements are limited to the blood velocity. In particular, 4D-MRI provides a measurement of the velocity field in the whole vessel. A natural question is hence to reconstruct the RPD from these velocity measurements. We refer to [6] for a review on direct based estimation methods for this problem. The purpose of this example is to illustrate how the method introduced in Section 3 can be used to estimate the RPD from full velocity measurements.

We assume that blood flow is described by the Navier-Stokes equations and that we have velocity measurements in the whole domain Ω (see Figure 3) at a given set of time instants. We denote by $(0, T)$ the time interval,

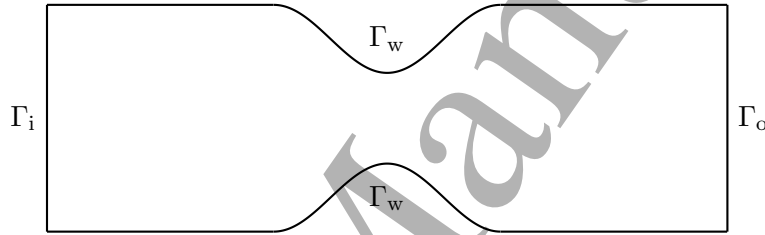


Figure 3: Geometric description of the domain Ω representing a stenotic blood vessel

by N the number of measurements instants and set the time-step length to $\Delta t := \frac{T}{N-1}$. For all $0 \leq n \leq N-1$, the symbol u_M^n stands for the measured velocity at time $t_n = n\Delta t$. Then, for all $0 \leq n \leq N-2$, we consider the following Oseen type equation in terms of (u^n, p^n) :

$$\begin{cases} (u_M^n \cdot \nabla)u^n - 2\nu \nabla \cdot \varepsilon(u^n) + \nabla p^n = -\frac{u_M^{n+1} - u_M^n}{\Delta t} & \text{in } \Omega, \\ \nabla \cdot u^n = 0 & \text{in } \Omega. \end{cases} \quad (30)$$

Note that no boundary data is prescribed in (30), which can be cumbersome in practice since the measured velocity u_M^n is not necessarily divergence free (and hence incompatible with Dirichlet data on the whole boundary $\partial\Omega$). We hence propose to estimate u^n and p^n (up to a constant) from the data assimilation problem (11), with f and a (in the definition (10) of A) given respectively by

$$f = -\frac{u_M^{n+1} - u_M^n}{\Delta t}, \quad a(u, v) = \int_{\Omega} ((u_M^n \cdot \nabla)u) \cdot v + \nu \int_{\Omega} \varepsilon(u) : \varepsilon(v).$$

Note that, here, the measurement and target sets coincide, $\omega_M = \omega_T = \Omega$, so that the estimated velocity field u^n has to be seen as a physically driven regularization of the full velocity measure u_M^n . Yet, the main target is to estimate the RPD, defined by the following quantity:

$$\delta p = \frac{1}{|\Gamma_i|} \int_{\Gamma_i} p - \frac{1}{|\Gamma_o|} \int_{\Gamma_o} p.$$

In order to investigate this new approach, we consider a two-dimensional version of the test case reported in [6, Section 6]. The stenotic blood vessel represented in Figure 3 corresponds to a contraction of 60%. The radii of inlet and outlet are 1 cm, the length of the vessel is 6 cm and the dynamic viscosity is given by $\nu = 0.035$ Poise. Synthetic measurements are first generated by numerically solving the incompressible Navier-Stokes system

$$\begin{cases} \partial_t u + (u \cdot \nabla)u - 2\nu \nabla \cdot \varepsilon(u) + \nabla p = 0 & \text{in } \Omega \times (0, T), \\ \nabla \cdot u = 0 & \text{in } \Omega \times (0, T), \end{cases} \quad (31)$$

with the following boundary and initial conditions:

$$\begin{cases} u = 0 & \text{on } \Gamma_w \times (0, T), \\ u = \left((-60(y^2 - 1) \sin\left(\frac{5\pi}{2}t\right), 0 \right) & \text{on } \Gamma_i \times (0, T), \\ 2\nu \varepsilon(u)n - pn = 0 & \text{on } \Gamma_o \times (0, T), \\ u(\cdot, 0) = 0 & \text{in } \Omega. \end{cases} \quad (32)$$

This direct problem (31)-(32) is discretized in space by continuous piecewise affine finite element approximations based on the SUPG/PSPG stabilization method. The time discretization consists in a backward Euler scheme with a semi-implicit treatment of the convective term. A standard backflow stabilization term is also applied on the outlet boundary Γ_o in order to guarantee the overall stability of the numerical scheme (see, e.g., [15]). The discretization parameters are set to $\Delta t = 0.002$ s and $h = 0.01$ cm. This space-time grid generates a set of synthetic velocity measurements which can be perturbed either by noise or by space-time subsampling.

Figure 4 represents the estimate RPD with the same discretization parameters as for the direct problem (no subsampling). When the data are unperturbed, we see that the reconstructed curve is perfectly superimposed with the exact curve (Figure 4, left). With a 10% Gaussian noise, we observe that the reconstructed curve (which corresponds to the mean curve

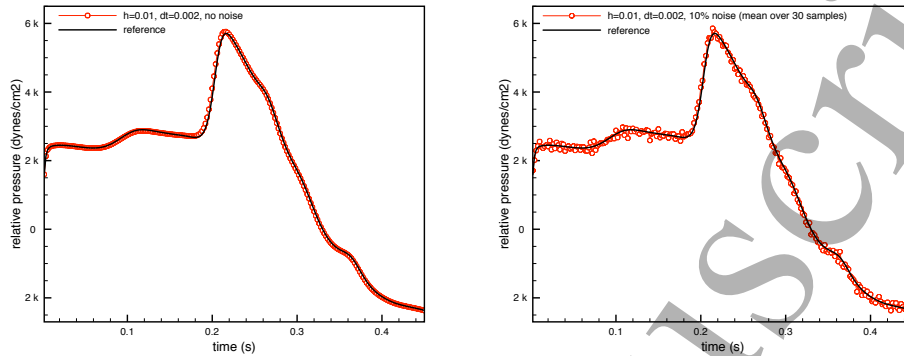


Figure 4: Left: Noise free data, right: 10% Gaussian noise on the data with exact sampling. The exact RPD is represented in full line whereas the reconstructed RPD is represented in dotted line.

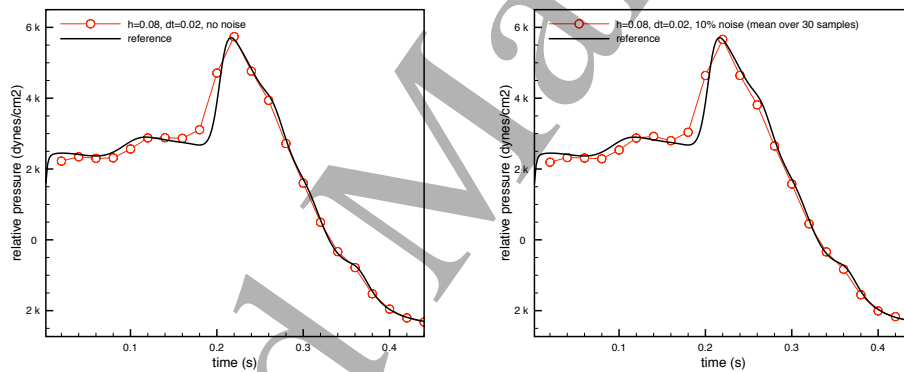


Figure 5: Left: Time subsampling of 0.02 s, right: Space subsampling of 0.08 cm. The exact RPD is represented in full line whereas the reconstructed RPD is represented in dotted line.

obtained from 30 tests with variable noises) succeeds in following accurately the variations of the reference data (Figure 4, right).

In Figure 5, the measurements are perturbed by a subsampling both in time and in space (the time step is 10 times larger and the mesh size is 8 times larger). We then solve the data assimilation problem with the time step or the mesh size corresponding to this subsampling. Figure 5 shows that the proposed approach is able to provide a reasonable estimation of the RPD with and without noise (10% Gaussian noise). In particular, we can clearly observe that the RPD peak is well captured in both cases.

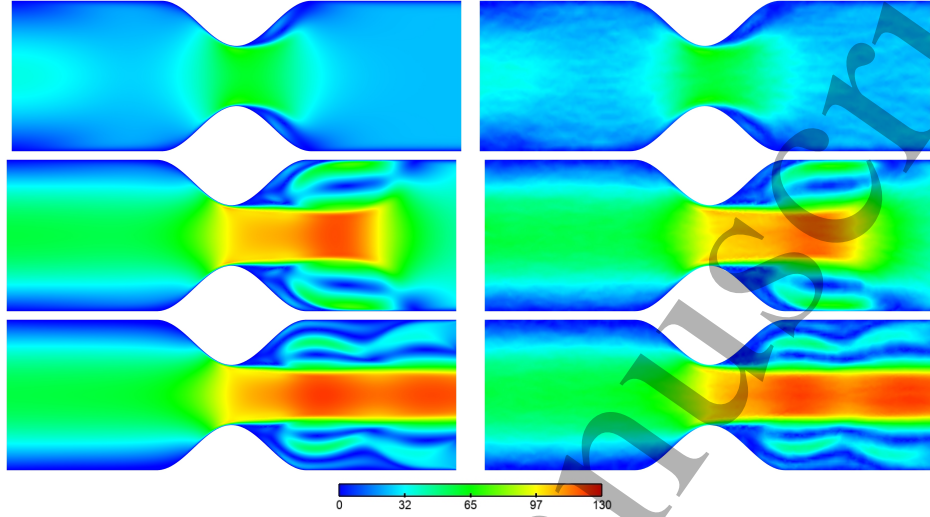


Figure 6: Velocity magnitude at $t = 0.082, 0.162, 0.242$ (from top to bottom). Right: reference. Left: reconstruction with space-time subsampling and 10% of Gaussian noise.

A Proof of Corollary 2.1

Let us first assume that there exist $x_0 \in \omega_M$ and $0 < R_1 < R_2 < R_3 \leq R_0$ such that $B_{R_1}(x_0) \subset \omega_M$, $\omega_T \subset B_{R_2}(x_0)$, $B_{R_0}(x_0) \subset \subset \Omega$ and $R_1/R_3 < R_2/R_3 < \tilde{R}$ where \tilde{R} is defined in Theorem 2.1.

According to Assumption A, problem (6), with homogeneous Dirichlet boundary conditions, admits a unique solution that we denote $(\tilde{u}, \tilde{p}) \in V_0 \times L_0$. Then $(\tilde{w}, \tilde{y}) := (u - \tilde{u}, p - \tilde{p})$ satisfies (1) with $f = 0$. Using the interior regularity of solution of Stokes problem (see for instance [39]), $(\tilde{w}, \tilde{y}) \in [H^1(B_{R_0}(x_0))]^d \times H^1(B_{R_0}(x_0))$. We may then write

$$|u|_{\omega_T} \leq |\tilde{u}|_{\omega_T} + |\tilde{w}|_{\omega_T}. \quad (33)$$

For the first term in the right hand side, we use that (\tilde{u}, \tilde{p}) satisfies the stability inequality (7):

$$|\tilde{u}|_{\omega_T} \lesssim (\|f\|_{V'_0} + \|g\|_L).$$

Here and in the sequel, we will frequently use the notation $a \lesssim b$ for $a \leq Cb$ for some $C > 0$.

For the second term in the right hand side of (33), applying Theorem

2.1, we get that (\tilde{w}, \tilde{y}) satisfies (8) and thus:

$$|\tilde{w}|_{\omega_T} \leq \|\tilde{w}\|_{[L^2(B_{R_2}(x_0))]^d} \lesssim \|\tilde{w}\|_{[L^2(B_{R_3}(x_0))]^d}^{1-\tau} \|\tilde{w}\|_{[L^2(B_{R_1}(x_0))]^d}^\tau \lesssim \|\tilde{w}\|_L^{1-\tau} |\tilde{w}|_{\omega_M}^\tau.$$

We now revert back to u in the right hand side:

$$\begin{aligned} |\tilde{w}|_{\omega_T} &\lesssim (\|\tilde{u}\|_L + \|u\|_L)^{1-\tau} (|\tilde{u}|_{\omega_M} + |u|_{\omega_M})^\tau \\ &\lesssim (\|f\|_{V'_0} + \|g\|_L + \|u\|_L)^{1-\tau} (\|f\|_{V'_0} + \|g\|_L + |u|_{\omega_M})^\tau. \end{aligned}$$

We conclude the proof by collecting the estimates for \tilde{u} and \tilde{w} .

If ω_M and ω_T do not satisfy the assumptions for the construction of the balls $B_{R_1}(x_0)$ and $B_{R_0}(x_0)$, we introduce a finite sequence of intermediate balls in order to link ω_T to ω_M (as it is done for instance in [37]) and we get again the estimate.

References

- [1] Giovanni Alessandrini, Luca Rondi, Edi Rosset, and Sergio Vessella. The stability for the Cauchy problem for elliptic equations. *Inverse Problems*, 25(12):123004, 47, 2009.
- [2] Didier Auroux, Patrick Bansart, and Jacques Blum. An evolution of the back and forth nudging for geophysical data assimilation: application to Burgers equation and comparisons. *Inverse Probl. Sci. Eng.*, 21(3):399–419, 2013.
- [3] Mehdi Badra, Fabien Caubet, and Jérémie Dardé. Stability estimates for Navier-Stokes equations and application to inverse problems. *Discrete Contin. Dyn. Syst. Ser. B*, 21(8):2379–2407, 2016.
- [4] Andrea Ballerini. Stable determination of an immersed body in a stationary Stokes fluid. *Inverse Problems*, 26(12):125015, 25, 2010.
- [5] Mourad Bellassoued, Oleg Imanuvilov, and Masahiro Yamamoto. Carleman estimate for the Navier-Stokes equations and an application to a lateral Cauchy problem. *Inverse Problems*, 32(2):025001, 23, 2016.
- [6] Cristóbal Bertoglio, Rodolfo Nuñez, Felipe Galarce, David Nordsletten, and Axel Osses. Relative pressure estimation from velocity measurements in blood flows: state-of-the-art and new approaches. *Int. J. Numer. Methods Biomed. Eng.*, 34(2):e2925, 16, 2018.

- 1
2
3
4
5
6
7
8 [7] Muriel Boulakia, Anne-Claire Egloffé, and Céline Grandmont. Stability
9 estimates for the unique continuation property of the Stokes system
10 and for an inverse boundary coefficient problem. *Inverse Problems*,
11 29(11):115001, 21, 2013.
12
13 [8] L. Bourgeois. A mixed formulation of quasi-reversibility to solve the
14 Cauchy problem for Laplace’s equation. *Inverse Problems*, 21(3):1087–
15 1104, 2005.
16
17 [9] Laurent Bourgeois and Jérémie Dardé. A quasi-reversibility approach to
18 solve the inverse obstacle problem. *Inverse Probl. Imaging*, 4(3):351–
19 377, 2010.
20
21 [10] Laurent Bourgeois and Jérémie Dardé. The “exterior approach” to solve
22 the inverse obstacle problem for the Stokes system. *Inverse Probl. Imag-*
23 *ing*, 8(1):23–51, 2014.
24
25 [11] Laurent Bourgeois and Arnaud Recoquillay. A mixed formulation of the
26 Tikhonov regularization and its application to inverse PDE problems.
27 *ESAIM Math. Model. Numer. Anal.*, 52(1):123–145, 2018.
28
29 [12] James H. Bramble, Raytcho D. Lazarov, and Joseph E. Pasciak. A
30 least-squares approach based on a discrete minus one inner product for
31 first order systems. *Math. Comp.*, 66(219):935–955, 1997.
32
33 [13] James H. Bramble, Raytcho D. Lazarov, and Joseph E. Pasciak. Least-
34 squares for second-order elliptic problems. *Comput. Methods Appl.*
35 *Mech. Engrg.*, 152(1-2):195–210, 1998. Symposium on Advances in
36 Computational Mechanics, Vol. 5 (Austin, TX, 1997).
37
38 [14] F. Brezzi and J. Pitkäranta. On the stabilization of finite element
39 approximations of the Stokes equations. In *Efficient solutions of elliptic*
40 *systems (Kiel, 1984)*, volume 10 of *Notes Numer. Fluid Mech.*, pages
41 11–19. Friedr. Vieweg, Braunschweig, 1984.
42
43 [15] Ch.-H. Bruneau and P. Fabrie. Effective downstream boundary condi-
44 tions for incompressible navierstokes equations. *International Journal*
45 *for Numerical Methods in Fluids*, 19(8):693–705, 1994.
46
47 [16] A. L. Bukhgeim and M. V. Klivanov. Uniqueness in the large of a
48 class of multidimensional inverse problems. *Dokl. Akad. Nauk SSSR*,
49 260(2):269–272, 1981.
50
51
52
53
54
55
56
57
58
59
60

- 1
2
3
4
5
6
7
8 [17] E. Burman, M. Nechita, and L. Oksanen. A stabilized finite element
9 method for inverse problems subject to the convection–diffusion equa-
10 tion. Part 1: Diffusion dominated regime. in preparation 2018.
- 11
12 [18] E. Burman, M. Nechita, and L. Oksanen. Unique continuation for the
13 Helmholtz equation using stabilized finite element methods. *ArXiv e-*
14 *prints*, October 2017.
- 15
16 [19] Erik Burman. Stabilized finite element methods for nonsymmetric,
17 noncoercive, and ill-posed problems. Part I: Elliptic equations. *SIAM*
18 *J. Sci. Comput.*, 35(6):A2752–A2780, 2013.
- 19
20 [20] Erik Burman. Error estimates for stabilized finite element methods
21 applied to ill-posed problems. *C. R. Math. Acad. Sci. Paris*, 352(7-
22 8):655–659, 2014.
- 23
24 [21] Erik Burman. Stabilised finite element methods for ill-posed problems
25 with conditional stability. In *Building bridges: connections and chal-*
26 *lenges in modern approaches to numerical partial differential equations*,
27 volume 114 of *Lect. Notes Comput. Sci. Eng.*, pages 93–127. Springer,
28 [Cham], 2016.
- 29
30 [22] Erik Burman and Peter Hansbo. Stabilized nonconforming finite el-
31 ement methods for data assimilation in incompressible flows. *Math.*
32 *Comp.*, 87(311):1029–1050, 2018.
- 33
34 [23] Erik Burman, Peter Hansbo, and Mats G. Larson. Solving ill-posed
35 control problems by stabilized finite element methods: an alternative
36 to Tikhonov regularization. *Inverse Problems*, 34(3):035004, 36, 2018.
- 37
38 [24] Erik Burman, Jonathan Ish-Horowicz, and Lauri Oksanen. Fully dis-
39 crete finite element data assimilation method for the heat equation.
40 *ESAIM: M2AN*, 2018.
- 41
42 [25] Erik Burman and Lauri Oksanen. Data assimilation for the heat equa-
43 tion using stabilized finite element methods. *Numer. Math.*, 2018.
- 44
45 [26] Marta D’Elia and Alessandro Veneziani. Uncertainty quantification for
46 data assimilation in a steady incompressible Navier-Stokes problem.
47 *ESAIM Math. Model. Numer. Anal.*, 47(4):1037–1057, 2013.
- 48
49 [27] Daniele Antonio Di Pietro and Alexandre Ern. *Mathematical aspects of*
50 *discontinuous Galerkin methods*, volume 69 of *Mathématiques & Appli-*
51
52
53
54
55
56
57
58
59
60

- 1
2
3
4
5
6
7
8 *cations (Berlin) [Mathematics & Applications]*. Springer, Heidelberg,
9 2012.
- 10
11 [28] Alexandre Ern and Jean-Luc Guermond. *Theory and practice of fi-*
12 *nite elements*, volume 159 of *Applied Mathematical Sciences*. Springer-
- 13 Verlag, New York, 2004.
- 14
15 [29] Caroline Fabre and Gilles Lebeau. Prolongement unique des solutions
16 de l'équation de Stokes. *Comm. Partial Differential Equations*, 21(3-
- 17 4):573–596, 1996.
- 18
19 [30] Ciprian Foias, Cecilia F. Mondaini, and Edriss S. Titi. A discrete data
20 assimilation scheme for the solutions of the two-dimensional Navier-
- 21 Stokes equations and their statistics. *SIAM J. Appl. Dyn. Syst.*,
22 15(4):2109–2142, 2016.
- 23
24 [31] F. Hecht. New development in FreeFem++, *J. Numer. Math.*, 20(3-
- 25 4):251–265, 2012.
- 26
27 [32] James E. Hoke and Richard A. Anthes. The initialization of numerical
28 methods by a dynamic-initialization technique. *Monthly Weather*
29 *Review*, 1976.
- 30
31 [33] O. Yu. Imanuvilov and M. Yamamoto. Global uniqueness in inverse
32 boundary value problems for the Navier-Stokes equations and Lamé
33 system in two dimensions. *Inverse Problems*, 31(3):035004, 46, 2015.
- 34
35 [34] O. Yu. Imanuvilov and M. Yamamoto. Remark on boundary data for
36 inverse boundary value problems for the Navier-Stokes equations [Ad-
- 37 dendum to MR3319370]. *Inverse Problems*, 31(10):109401, 4, 2015.
- 38
39 [35] Rajaraman Prathish K., Manteuffel T. A., Belohlavek M., and Heys Jef-
- 40 frey J. Combining existing numerical models with data assimilation us-
- 41 ing weighted least squares finite element methods. *International Jour-*
42 *nal for Numerical Methods in Biomedical Engineering*, 33(1):e02783,
43 2017. e02783 CNM-Oct-15-0192.R1.
- 44
45 [36] Ching-Lung Lin, Gunther Uhlmann, and Jenn-Nan Wang. Optimal
46 three-ball inequalities and quantitative uniqueness for the Stokes sys-
- 47 tem. *Discrete Contin. Dyn. Syst.*, 28(3):1273–1290, 2010.
- 48
49 [37] Luc Robbiano. Théorème d'unicité adapté au contrôle des solutions
50 des problèmes hyperboliques. *Comm. Partial Differential Equations*,
51 16(4-5):789–800, 1991.
- 52
53
54
55
56
57
58
59
60

- 1
2
3
4
5
6
7
8 [38] Y. Sasaki. Some basic formalisms in numerical variational analysis. *Monthly Weather Review*, 98(12):875–883, 1970.
- 9
10
11 [39] Gregory Seregin. *Lecture notes on regularity theory for the Navier-Stokes equations*. World Scientific Publishing Co. Pte. Ltd., Hackensack, NJ, 2015.
- 12
13
14
15 [40] O. Talagrand and P. Courtier. Variational assimilation of meteorological observations with the adjoint vorticity equation. i: Theory. *Quarterly Journal of the Royal Meteorological Society*, 113(478):1311–1328, 1987.
- 16
17
18
19
20 [41] Olivier Talagrand. On the mathematics of data assimilation. *Tellus*, 33(4):321–339, 1981.
- 21
22
23 [42] Sergiy Zhuk and Olexander Nakonechnii. Minimax state estimates for abstract Neumann problems. *Minimax Theory Appl.*, 3(1):1–21, 2018.
- 24
25
26
27
28
29
30
31
32
33
34
35
36
37
38
39
40
41
42
43
44
45
46
47
48
49
50
51
52
53
54
55
56
57
58
59
60